Variations in Streamflow Response to Large Hurricane-Season Storms in a Southeastern U.S. Watershed

XING CHEN, MUKESH KUMAR, AND BRIAN L. MCGLYNN

Nicholas School of the Environment, Duke University, Durham, North Carolina

(Manuscript received 6 March 2014, in final form 19 July 2014)

ABSTRACT

Floods caused by hurricane storms are responsible for tremendous economic and property losses in the United States. To minimize flood damages associated with large hurricane-season storms, it is important to be able to predict streamflow amount in response to storms for a range of hydroclimatological conditions. However, this is challenging considering that streamflow response exhibits appreciable variability even for hurricane-season storms that deliver similar precipitation amounts. As such, better estimates of event responses require refined understanding of the causes of flood response variability. Here, a physically based, distributed hydrologic model and supporting hydrologic datasets are used to identify and evaluate dominant hydrologic controls on streamflow amount variability. The analysis indicates that variability in flood response in the Lake Michie watershed is primarily driven by antecedent soil moisture conditions near the land surface and evapotranspiration during postevent streamflow recession periods, which in turn is a function of precipitation history and prevailing vegetation and meteorological conditions. Presented results and ensuing analyses could help prioritize measurements during observation campaigns and could aid in risk management by providing look-up diagrams to quickly evaluate flood responses given prior information about hurricane storm size.

1. Introduction

Hurricanes and tropical storms are major geophysical disaster-causing agents, which account for billions of dollars in annual property damages (Changnon 2009; Dale et al. 2001; Emanuel et al. 2008; Emanuel 1987; Saunders et al. 2000). In the United States alone, average annual losses caused by these storms exceeded $2.6 billion per year for the period 1949–2006 (Changnon 2009; Changnon and Changnon 1992). Most of these storms originate in the Atlantic Ocean between June and November (Changnon 2009) and cause extensive losses in the southeastern states including Louisiana, Florida, Georgia, South Carolina, and North Carolina. In North Carolina, where approximately 350 hurricanes have hit since 1667 (NCDC 2014; SCONC 2014a; Hardy and Carney 1963; Carney and Hardy 1967), these storms have caused hundreds of fatalities and billions of dollars in property damages (Blake et al. 2007; NOAA 2013a,b). A large percentage of these losses have been due to flooding from intense storms (Ashley and Ashley 2008; NOAA 2013a). To the dismay of water resource and risk managers, risks associated with remnant hurricanes and tropical storms are expected to increase in the future, as global warming is predicted to result in an increased intensity of tropical disturbances (Easterling et al. 2000; Elsner 2007; Goldenberg et al. 2001; Knutson and Tuleya 2004; Landsea 2007; Mann and Emanuel 2006; Pielke et al. 2005; Salinger 2005; Webster et al. 2005).

Flooding-related damages due to hurricane or other tropical-disturbance storms can be considerably reduced if accurate prediction of streamflow response to these storms can be made. Prediction of flood responses to precipitation is nontrivial because they reflect more than just rain event size. For example, streamflow data from the Lake Michie watershed (LMW) in North Carolina (Fig. 1, Table 1) shows that streamflow response to large, similar-magnitude (in terms of precipitation amount) hurricane-season storms can be significantly different. Note that hurricane-season storms in this paper indicate storms that have hurricane or other tropical-disturbance origins and happen between June and November. Events are defined to span from the start

Corresponding author address: Mukesh Kumar, Nicholas School of the Environment, Duke University, 450 Research Dr., LSRC A207A, Durham, NC 27708.
E-mail: mukesh.kumar@duke.edu

DOI: 10.1175/JHM-D-14-0044.1

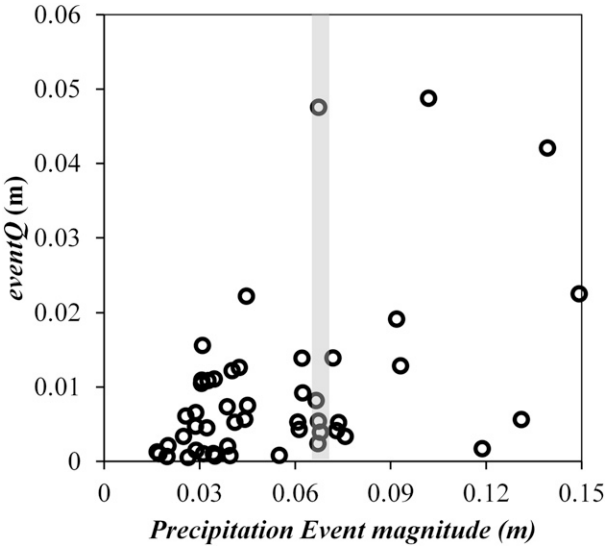

FIG. 1. Observed streamflow responses due to large hurricane-season events (magnitude larger than 0.016 m).

of precipitation to the time after which there is no rainfall for at least 6 h. The terms "event size" and "storm size" have been used interchangeably throughout the paper and refer to the amount of precipitation delivered during the storm event. Enormous variability in streamflow response is highlighted by dots falling within the vertical shaded bar in Fig. 1, where storms of size of approximately 0.07 m are observed to generate streamflow with magnitudes varying by as much as 250% around the mean. Additional details of these events are in rows 2, 5, 13, and 19 in Table 1 (identified by asterisks). The flow magnitude in response to an event (in Fig. 1) is defined as the total flow amount from the beginning of an event to the time when the recession limb flattens after the end of that single storm. The observed variability of flood response suggests that, in addition to storm event size, other transient controls such as evolving land surface characteristics and hydrologic states may have a significant influence on flow responses to storm events. While previous studies have investigated contributing factors to streamflow generation during and immediately after isolated hurricane storms (Castillo et al. 2003; Elsenbeer et al. 1995; Sturdevant-Rees et al. 2001; Tramblay et al. 2010; Wood 1976), their influence on the variability of flood response from one large hurricane-season storm to the other, both intra- and interannually, has gone largely unreported. This gap in knowledge is partially attributable to the challenge associated with measurement of multiple hydrologic states over long periods of time. Because hurricanes and tropical storms are not a year-wise phenomenon, tracking the role of controls on response variability would require multiyear datasets and detailed investigations. This is expected to be a resource-intensive task, as understanding of the influence of controls on the variability of flood response would ideally require collocated observations within a watershed that track partitioning across the hydrologic continuum, including surface flow, evapotranspiration et, vadose zone soil moisture, and groundwater response across multiple hurricane-season storms.

The goal of this paper is to identify the causes of variability in flood response amount to large hurricane-season storms. Variability in response from one event to another, even if the events deliver similar precipitation amounts, is caused mainly by differences in transient controls such as meteorological and antecedent hydrological conditions. Therefore, we specifically evaluate controls on streamflow variability from one storm event to next. The streamflow response discussed in this paper refers to the total discharge amount, rather than the peak discharge. Our case study utilizes publicly available observation data in synergy with a physically based numerical watershed model and demonstrates the wide applicability of the approach in data-poor regions.

2. Data and methods

a. Study area and datasets

We selected the Lake Michie watershed in North Carolina as the study site to analyze the causes of variability in flood response to large hurricane-season storms. LMW is frequently struck by hurricane-season storms originating from the Atlantic Ocean. The watershed area is 432.8 km^2 and is part of the Neuse River basin. Streamflow output from the watershed is delivered into the Lake Michie reservoir, which has served as the primary water supply for the city of Durham (population of 279 641 in 2012) since 1929 (Weaver 1994). Varied streamflow response to hurricane-season storms poses a significant challenge for effective reservoir management, water resource allocation, and risk assessment in the watershed and thus underscores the need for better understanding of flood response.

The LMW is characterized by northwest-to-southeast-oriented valleys, with elevation ranging from 87 to 270 m MSL (Fig. 2d). Most of the watershed consists of gentle to moderately rolling hills with some steep, narrow valleys immediately upstream of the Lake Michie reservoir (Weaver 1994). Upland slopes range from 0° to 36°. We used 30-m-resolution digital elevation model grid data from the U.S. Geological Survey (USGS; http://nationalmap.gov/viewer.html) for analyses. Climate in the watershed is characterized by long, hot, humid summers and short, mild winters with transitional

TABLE 1. Named 42 largest hurricane-season storms in North Carolina during 1985–2012. In the second column, asterisks identify events that have been highlighted by shading in Fig. 1. In the last column, variables *d* and et identify the dominant control on streamflow response to large hurricane-season storms.

No.	Event name	Event date	Event size (m)	Streamflow response size (m)	Antecedent soil moisture	Dominant control
1	Tropical Storm Juan	30 Oct 1985	0.108	0.033	0.21	*d*
2 (C)	Tropical Storm Kate*	20 Nov 1985	0.067	0.044	0.76	*d*
3	Hurricane Charley	16 Aug 1986	0.092	0.022	0.31	et
4	Tropical Depression Nine	3 Sep 1987	0.098	0.027	0.03	*d*
5	Tropical Depression Chris*	28 Aug 1988	0.067	0.008	0.01	*d*
6	Tropical Storm Isaac	2 Oct 1988	0.061	0.007	0.11	*d*
7	Tropical Storm Barry	15 Jul 1989	0.052	0.006	0.20	et
8 (B)	Hurricane Klaus	10 Oct 1990	0.101	0.018	0.09	*d*
9	Hurricane Lili	22 Oct 1990	0.083	0.043	0.47	*d*
10	Tropical Storm Ana	24 Sep 1991	0.076	0.015	0.17	*d*
11	Tropical Depression Two	25 Jul 1994	0.064	0.001	0.22	et
12	Hurricane Allison	9 Jun 1995	0.052	0.015	0.46	et
13 (D)	Tropical Depression Jerry*	25 Aug 1995	0.067	0.009	0.50	et
14	Hurricane Opal	3 Oct 1995	0.073	0.013	0.14	*d*
15	Tropical Storm Sebastien	20 Oct 1995	0.054	0.018	0.30	*d*
16	Hurricane Fran	3 Sep 1996	0.063	0.001	0.09	*d*
17	Hurricane Danny	22 Jul 1997	0.060	0.004	0.11	*d*
18	Major Hurricane Erika	9 Sep 1997	0.064	0.010	0.00	*d*
19	Hurricane Earl*	3 Sep 1998	0.068	0.006	0.05	*d*
20	Hurricane Dennis	25 Aug 1999	0.055	0.003	0.05	*d*
21	Hurricane Dennis	4 Sep 1999	0.149	0.071	0.17	*d*
22	Hurricane Floyd	14 Sep 1999	0.115	0.060	0.31	et
23 (A)	Tropical Storm Harvey	27 Sep 1999	0.102	0.036	0.43	*d*
24	Tropical Storm Gustav	29 Aug 2002	0.074	0.014	0.35	et
25	Tropical Storm Kyle	10 Oct 2002	0.140	0.077	0.06	*d*
26	Tropical Depression Bill	1 Jul 2003	0.054	0.019	0.49	et
27	Hurricane Isabel	18 Sep 2003	0.055	0.010	0.21	*d*
28	Hurricane Juan	22 Sep 2003	0.053	0.023	0.55	et
29	Tropical Storm Bonnie	13 Aug 2004	0.062	0.007	0.38	et
30	Tropical Depression Gaston	29 Aug 2004	0.060	0.017	0.19	et
31	Tropical Storm Alberto	13 Jun 2006	0.051	0.016	0.41	et
32	Tropical Storm Ernesto	30 Aug 2006	0.073	0.006	0.01	*d*
33	Hurricane Isaac	5 Oct 2006	0.052	0.014	0.30	*d*
34	Hurricane Noel	24 Oct 2007	0.119	0.026	0.06	*d*
35	Major Hurricane Gustav	25 Aug 2008	0.131	0.049	0.04	*d*
36	Hurricane Hanna	5 Sep 2008	0.109	0.075	0.25	et
37	Tropical Depression One	4 Jun 2009	0.072	0.015	0.15	et
38	Hurricane Ida	10 Nov 2009	0.139	0.058	0.35	*d*
39	Hurricane Igor	26 Sep 2010	0.151	0.048	0.02	*d*
40	Hurricane Irene	5 Sep 2011	0.061	0.010	0.01	*d*
41	Tropical Storm Debby	9 Jul 2012	0.057	0.008	0.17	et
42	Hurricane Sandy	17 Sep 2012	0.061	0.004	0.08	*d*

seasons (Kopec and Clay 1975). During the years 1985–2012, average monthly temperature in the watershed ranged from 5°C in January to 35°C in July, while annual precipitation ranged from 802 to 1577 mm, with over half of the precipitation occurring during hurricane season (June–November). Annual runoff ratios (evaluated as the ratio of annual streamflow discharge and precipitation amount) for this period ranged from 0.11 to 0.46. Here we used hourly climate data (including precipitation, temperature, relative humidity, wind velocity, solar radiation, and vapor pressure) from the North American Land Data Assimilation System, phase 2 (NLDAS-2), meteorological forcings dataset (Xia et al. 2012). Spatial resolution of all the aforementioned forcing data is 1/8° or approximately 9.5 km in LMW (Mitchell et al. 2004). The watershed consists of 15 land cover types based on National Land Cover Data (MRLC 2013), and 56% of the watershed is covered by forest, while 34% of the total area is covered by shrubs. Forests in the watershed include deciduous, evergreen, and mixed conifer trees, while shrubs include scrub, hay, grassland, and crops. The percentage of developed area in the watershed

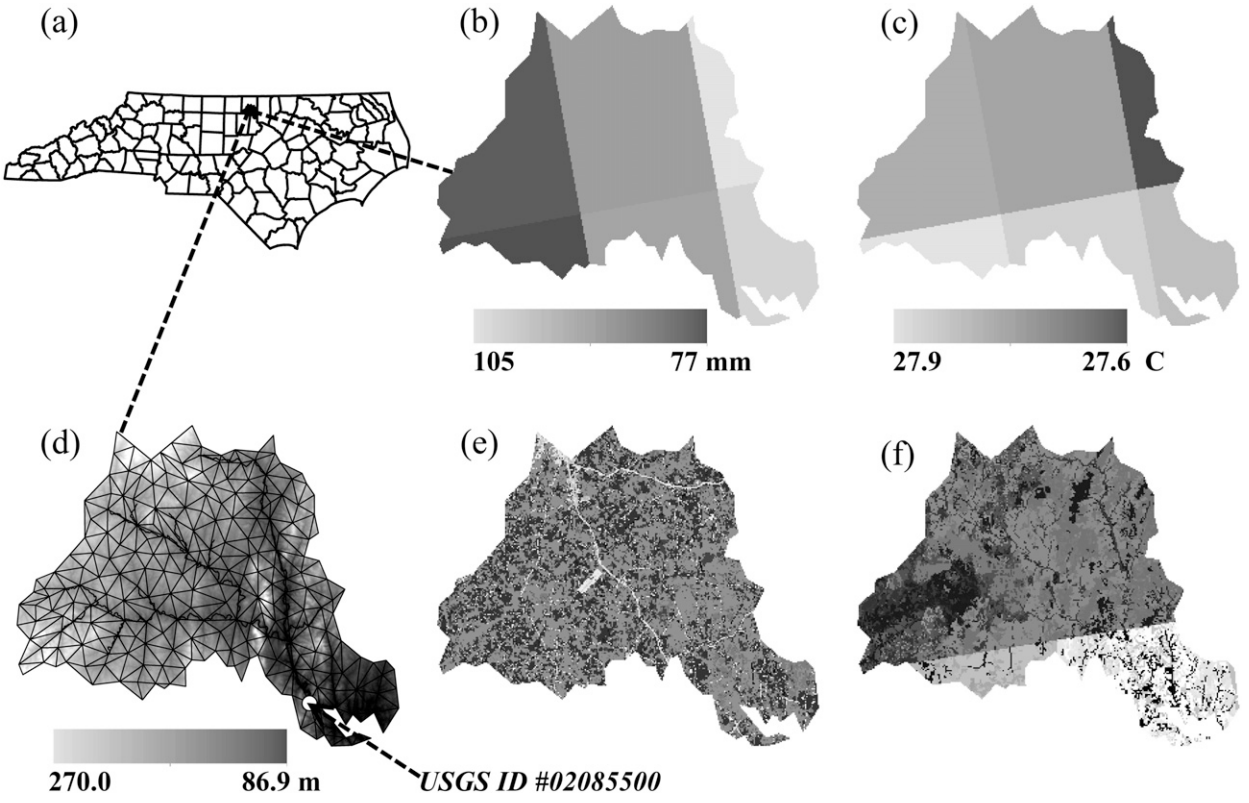

FIG. 2. (a) North Carolina county map, with LMW location (shown by black dot). (b) Precipitation (July 2002), (c) temperature (July 2002), (d) elevation, (e) land cover, and (f) soil map of LMW.

is approximately 9% of the total area. Soil Survey Geographic (SSURGO) data (Soil Survey Staff 2013) indicate that the watershed consists of 33 soil composition types, with majority of the area covered with loamy soils.

b. *Model description*

A physically based, spatially distributed hydrologic model, Penn State Integrated Hydrologic Model (PIHM; Kumar 2009; Kumar et al. 2009b; Qu and Duffy 2007), was used here to perform long-term integrated hydrologic simulations of streamflow and other coupled hydrologic states. PIHM employs a semidiscrete finite volume formulation to locally integrate partial differential equations of hydrologic processes to ordinary differential equations (ODEs) on each unstructured mesh element (Fig. 2d). The system of ODEs defined on all mesh elements were assembled and solved simultaneously with a stiff ODE solver using an implicit Newton–Krylov integrator. An adaptive time-stepping scheme is used for capturing model dynamics during a period of rapid changes in states, triggered usually by precipitation pulse. The control volume elements used to discretize the domain include triangular- and linear-shaped units, which represent land surface elements and rivers, respectively. These elements are projected downward to the bedrock (for land surface elements) or to the river bed (for river elements) to form prismatic or cuboidal elements, respectively, in 3D (Kumar 2009). The model was implemented on an unstructured mesh decomposition of the LMW (Fig. 2d), with 399 land elements (3D prismatic units) and 77 river segments (3D cuboidal units). Each land element was discretized into three layers: a top, relatively thin unsaturated zone with thickness of 0.25 m; an intermediate unsaturated zone that extends from 0.25 m to groundwater level; and a groundwater layer. The two lower layers have variable dimensions, as they depend on the evolving groundwater table depth GW. Each river unit was vertically discretized into two layers, with flowing river on the top and a groundwater zone below it. Processes simulated in PIHM include snowmelt, evapotranspiration (Penman–Monteith equation), interception (Rutter model), overland flow (2D diffusion wave equations), unsaturated zone infiltration (1D approximation of the Richards equation), groundwater flow (3D Richards equation), and streamflow (1D diffusive wave).

c. *Model parameterization, calibration, and validation*

A tightly coupled GIS framework, PIHMgis (Bhatt et al. 2008, 2014), was used to parameterize the model

domain using the aforementioned datasets (see section 2a). This includes defining relations between hydrographic units and their physical properties. For more details about the processes, parameters, and topology of domain discretization, readers are referred to Kumar et al. (2009a, 2010).

PIHM simulations were performed for 28 years (1985–2012), for which streamflow data are available for validation. Streamflow calibration was performed against observed hourly streamflow data at USGS site ID #2085500 (Fig. 2d), which lies 12.8 km above the Lake Michie reservoir. The calibration was performed for the year 2002, which received an annual precipitation of 1139 mm, the same as the average precipitation for the entire simulation period. The calibration process involved nudging hydrogeological parameters uniformly across the model domain (Refsgaard and Storm 1996) to match the baseflow magnitude and groundwater head distribution during dry periods and the rate of hydrograph decay during recession. Two calibration periods were chosen: 1) a summer period with no appreciable recharge (from late April to early June) and 2) a wet, cold period with substantial streamflow response to precipitation and relatively low evapotranspiration (from November to December). The calibration process involved first initializing PIHM with the water table at the land surface and then letting the model relax with no precipitation input until streamflow approaches zero. The simulated relaxation hydrograph was compared with observed streamflow during the first calibration period (identified above). Streamflow during this period was mostly dominated by base flow, which in turn was controlled by subsurface properties of the model domain. The goal of this initial model calibration step was to identify sets of hydrogeological properties, such as van Genuchten coefficients, macro and matrix porosities, and hydraulic conductivities, which would allow a reasonable match between modeled and observed base flow and groundwater head distributions. The second calibration step involved comparing the simulated relaxation rates with the observed values. Streamflow calibration results and corresponding model efficiencies in the calibration year are shown in Fig. 3a. The dynamics of streamflow variation between observed and modeled results are in reasonable agreement and are considered acceptable. Similar modeled and observed runoff ratios of 0.219 and 0.214, respectively (Table 2), also indicate reliable partitioning of the water budget. Furthermore, annual et estimation of 660 mm in this watershed is in good agreement with estimated results from a nearby heavily vegetated site (areal distance of 26.5 km from Lake Michie reservoir) in Duke Forest, where et was reported to range from 580 to 740 mm annually (Stoy et al. 2006).

Results of streamflow validation for 1985–2012 (Fig. 3b) show a Nash–Sutcliffe efficiency of 0.68 and coefficient of determination R^2 of 0.83 for daily data, 0.80 and 0.90 for monthly data, and 0.72 and 0.89 for yearly data. It is to be noted that the watershed does not have any operationally active groundwater wells within it that can be used to validate the temporal dynamics of groundwater. This level of data scarcity is neither surprising nor unusual and is typical for watersheds of this size. In fact, the density of USGS groundwater observation wells in the contiguous United States is less than one well per 6150 km^2 (http://waterdata.usgs.gov/nwis/inventory). However, single-instance groundwater depth data do exist at 36 locations within the watershed. Modeled groundwater elevation heads are compared to the observed data for respective dates to evaluate the ability of the model in capturing the spatial distribution of groundwater level (Jones et al. 2008). The results show good agreement between simulated and observed groundwater elevation heads with $R^2 = 0.89$ (Fig. 3c), indicating that the distribution of modeled total groundwater heads reasonably matches the observed data. Notably, the target metrics of the calibration strategy—the rate of hydrograph decay during cold period and the magnitude of base flow and spatial distribution of groundwater table depth during summer—differ from the validation metrics such as the match between simulated and observed streamflow time series and static groundwater table depths. The goal was to avoid simply fitting parameters to match observed data, while attempting to best represent the underlying behavior and response dynamics of the watershed. Since no soil moisture monitoring stations exist within the watershed, soil moisture data from the nearest Environment and Climate Observing Network (ECONet) site (SCONC 2014b) in Durham, which is 13 km south of the watershed, were used for validation. Because of the similarity in both timing and magnitude of the precipitation at the soil moisture site and that within the LMW, it is reasonable to expect that soil moisture dynamics at the ECONet site should show similar patterns to that in the LMW, especially at locations within the watershed that have the same land cover and soil type. It is to be noted the landscape slope was also very similar (~4.5°) at the two comparison sites. Modeled soil moisture deficits d at these locations (with same land cover and soil type as at the soil moisture monitoring site) within LMW are compared to observed data at the ECONet site for 2009–10 (Fig. 3d). The soil moisture deficit is defined as the fraction of pore space in the top 0.25 m of the subsurface that needs to be filled

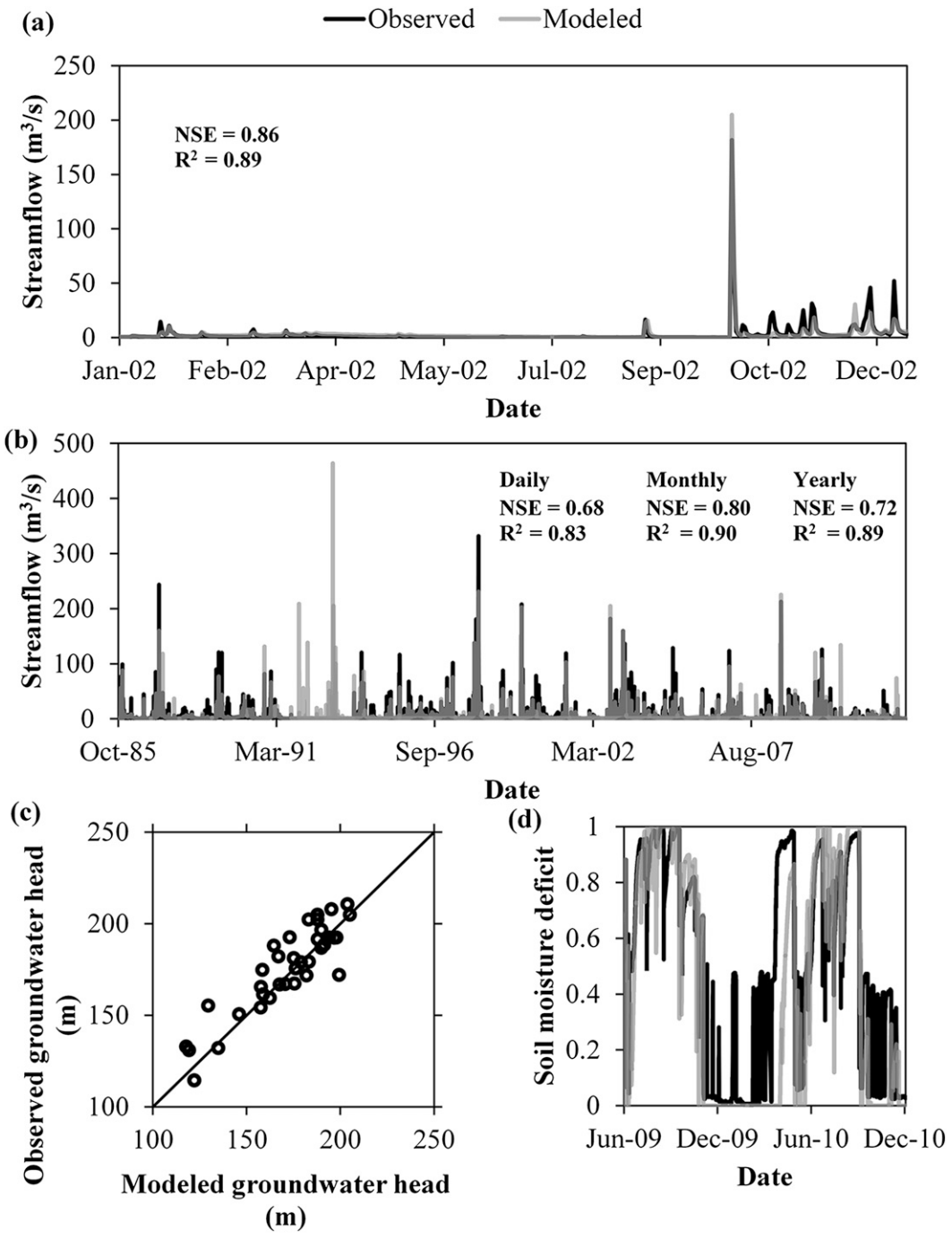

FIG. 3. Comparison of modeled and observed (a) discharge during calibration period, (b) discharge during the entire simulation period (1985–2012), (c) groundwater heads at 36 locations in LMW, and (d) soil moisture deficit at the ECONet site (soil moisture deficit = 1 − soil saturation).

by moisture before saturation occurs. Similar variations and ranges of moisture deficit between modeled and observed data suggest that the model was able to capture soil moisture dynamics to an acceptable degree. It is to be noted that soil moisture data after 2010 were not included in this analyses because of changes in instrument setup at the site and outstanding recalibration needs.

Since the focus of this paper is on the variability of streamflow response to large hurricane-season storms,

TABLE 2. Key water balance statistics for calibration year.

Precipitation (m)	Observed annual streamflow (m)	Simulated annual streamflow (m)	Total et (m)	Observed runoff ratio	Modeled runoff ratio
1.139	0.244	0.250	0.622	0.214	0.219

further confidence in the model result in this context was built by evaluating the ability of the model to simulate the order sequence of streamflow responses corresponding to large hurricane-season storms. Rank correlation coefficient of modeled and observed streamflow amounts rcc_Q corresponding to the top 50 hurricane-season storms (in terms of size) for the period 1985–2012 was calculated. For each event, streamflow amount under the hydrograph was calculated from the start of the event until the recession limb flattened. Flattening of the recession limb was identified by a flow difference of less than 80 m^3 in an hour, which is approximately 1% of the average flow rate from the watershed during hurricane season. Because some of these large events were immediately followed by other precipitation events at close time intervals, making it difficult to account for the streamflow response explicitly due to an event in consideration, rcc_Q was calculated only for events where streamflow contribution could be quantified without the convolved influence of following precipitation events. Rank correlation for these events was estimated to be equal to 0.81. This suggests that the PIHM simulations also reasonably captured the relative variability in streamflow response across multiple events.

The aforementioned validation results of streamflow, groundwater, soil moisture, and et, at scales ranging from events to seasons to decades, establishes sufficient confidence in the model performance for it to be used in evaluation of the role of controls on streamflow response variability to large hurricane-season storms.

d. *Understanding the role of controls on variable flood response from model results*

Variability in flood response to hurricane-season storms can be due to either differences in meteorological forcings or changes in watershed-response dynamics across different events. For events that deliver similar precipitation amounts, variations in hydrologic response (streamflow amount) can be caused by differences in transient controls such as antecedent hydrologic states and/or evolving watershed properties such as seasonal variation in ecohydrologic functions (e.g., transpiration and interception loss) of vegetation and meteorological forcings. To identify the controls on variability in flood response arising from large hurricane-season storms, we first quantified the streamflow contribution due to an event and then compared the hydrologic process contributions between events of similar sizes but considerably different responses. The first step was not trivial, considering that an observed streamflow discharge time series was often also composed of flow due to subsequent events that happened well before the influence of previous events on the streamflow hydrograph had subsided. To isolate the flow response generated only because of a particular precipitation event, we conducted event-scale PIHM simulations in addition to the long-term PIHM simulation (which was presented in section 2c). The event streamflow simulations were run from the start of the precipitation event to the time by which the generated streamflow recession limb flattened. Event simulations used observed meteorological forcings as inputs, while antecedent hydrologic conditions were set based on the results of the long-term simulation. Figure 4 shows simulated discharge obtained from the event simulation $event_Q$ and discharge per unit event size ($= event_Q/p$; where p is the precipitation magnitude), for the largest 50 hurricane-season storms (in terms of delivered precipitation amount) during the 28-yr simulation period. Large spread in flow response, even for events of similar sizes, is highlighted through two event pairs of magnitudes 0.067 m (events A and B), and 0.102 m (C and D), respectively (Table 1, Fig. 4a). For the 0.067- and 0.102-m storm sizes, $event_Q/p$ varies from 0.13 to 0.66 m m^{-1} and 0.18 to 0.35 m m^{-1}, respectively, suggesting that runoff ratios can vary by more than 100% in response to events of approximately the same size.

To understand the causes of differential streamflow response to similar-sized hurricane-season storms, hydrologic stores that vary markedly across the events were identified. For this, we considered the two event pairs with similar event size, identified earlier in Table 1 and Fig. 4. For each pair, the source of difference in streamflow response was first determined by comparing water partitions between different hydrologic stores (Table 3). It is to be noted that water partitions in all hydrologic stores were estimated from the start of the precipitation event to the time by which generated streamflow recession limb flattened. Because the summation of evapotranspirative loss, net change in storage del_S, and streamflow depth equals the precipitation magnitude, that is, $p = et + del_S + event_Q$, for events of

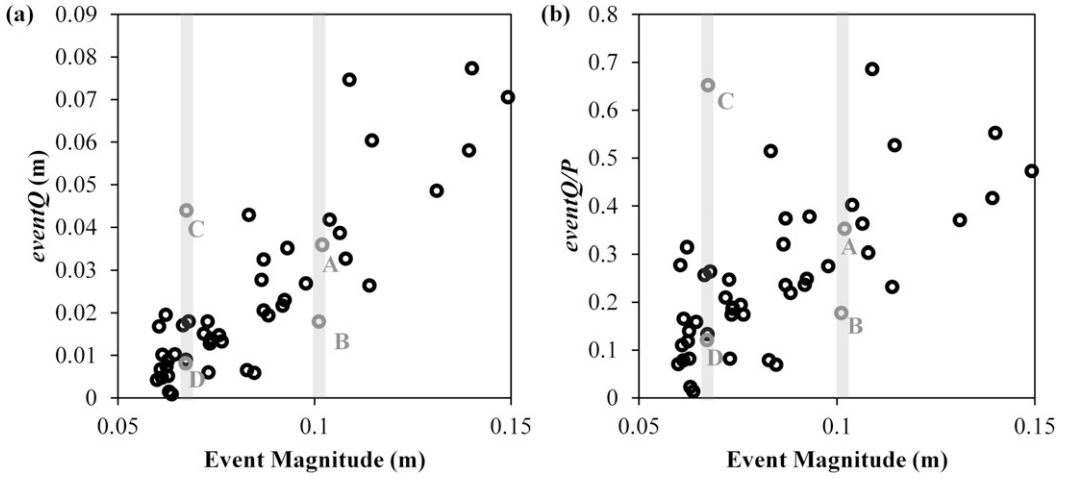

FIG. 4. Variation of (a) streamflow magnitude and (b) streamflow magnitude per unit event size, with event precipitation size for the largest 50 storm events in the hurricane season in LMW.

similar sizes, the difference in event_Q has to be due to differences in et and del_S terms. For events A and B, event_Q differs by 0.018 m. This difference is primarily attributable to the variation in net storage between events (0.015 m) as difference in et between the two events (i.e., Δet) is only 0.002. Larger Δdel_S could be due to differences in antecedent conditions during the events. In contrast, a difference of 0.035 m in event_Q between events C and D is predominantly due to the difference in et (0.024 m). This could be because of differences in meteorological conditions or transpiration and interception capability of vegetation between the two events. To identify the role of hydrologic controls on changes in hydrologic stores and hence the flood response, additional event simulations were conducted by removing the influence of controls one at a time. The role of these controls on a larger set of hurricane-season storms was subsequently tested by evaluating correlation between streamflow amount and effective precipitation size eff_p of hurricane-season events. It is to be noted that eff_p for an event was evaluated by calculating the difference between precipitation event size and the ''negative water store'' term, which includes evapotranspirative loss and the moisture storage deficit that needs to be filled before streamflow is generated. For example, eff_p for an event, during which the soil is completely saturated, is equal to the event precipitation magnitude ($p - \text{et}$). If the ground is unsaturated and streamflow due to a precipitation event is generated only after the topsoil layer gets saturated (after the moisture deficit has been filled), eff_p is evaluated as $p - (\text{et} + d)$. Henceforth, the correlation coefficient between event_Q and eff_p was compared to correlations between event_Q and p. A higher correlation between eff_p and event_Q would indicate that hydrologic stores used in the evaluation of eff_p play an important role in determining streamflow response. In contrast, a lower or negligible change in correlation coefficient with respect to correlation between p and event_Q would suggest that streamflow response is not sensitive enough to the concerned hydrologic stores that are used in evaluation of eff_p.

3. Results and discussion

a. *Role of watershed antecedent hydrologic conditions on variable streamflow response*

Comparison of water budget partitions for events A and B (see Table 3) shows that del_S during event B (0.069 m) was larger than during event A (0.054 m), thus indicating that difference in net storage (i.e., Δdel_S) played an important role in disparity in streamflow response between the two events. It is to be noted that del_S for an event is defined as the difference in total subsurface soil moisture content (both in unsaturated and saturated zone) between start and end of an event simulation. The marked difference in del_S (equal to 83% of the difference in streamflow response amount) between the two events could be attributed to larger moisture deficit in both the near-surface soil layer and the groundwater table for event B. To isolate the role of antecedent hydrologic conditions (and hence moisture deficit) on variability in flood response, an additional event simulation, A1, was conducted. The modeling configuration (watershed properties and meteorological conditions) of event simulation A1 was set exactly the same as that of event A; however, the antecedent

TABLE 3. Water partitioning across different water stores for event pairs (A, B) and (C, D) (identified in Fig. 4). A1, A2, and A3 are ancillary event simulations with exactly the same forcings as event A, but with all, only groundwater, or only surface soil moisture antecedent conditions being respectively identical to event B. C1, C2, and C3 are same as event C but they happen at same time as event D, have antecedent conditions identical to event D, and have both antecedent condition and timing of event D, respectively.

	Storm properties		Antecedent conditions		Water budget partition				Changes in water budget partitions between event pairs			
Event	Timing	p (m)	SS	GW (m)	event$_Q$ (m)	event$_Q/p$	del$_S$ (m)	et (m)	Δ	Δevent$_Q$ (m)	−Δdel$_S$ (m)	−Δet (m)
A	Sep	0.102	0.43	−9.2	0.036	0.35	0.054	0.012	B − A	−0.018	−0.015	−0.002
B	Oct	0.101	0.09	−10.3	0.018	0.18	0.069	0.014				
A1	Sep	0.102	0.09	−10.3	0.02	0.2	0.072	0.01	A1 − A	−0.016	−0.018	0.002
A2	Sep	0.102	0.43	−10.3	0.034	0.33	0.057	0.011	A2 − A	−0.002	−0.003	0.001
A3	Sep	0.102	0.09	−9.2	0.021	0.21	0.07	0.011	A3 − A	−0.015	−0.016	0.001
C	Nov	0.067	0.76	−6.5	0.044	0.66	0.016	0.007	D − C	−0.035	−0.011	−0.024
D	Aug	0.067	0.50	−7.5	0.009	0.13	0.027	0.031				
C1	Aug	0.067	0.76	−6.5	0.031	0.46	0.001	0.035	C1 − C	−0.013	0.015	−0.028
C2	Nov	0.067	0.50	−7.5	0.023	0.34	0.038	0.006	C2 − C	−0.021	−0.022	0.001
C3	Aug	0.067	0.50	−7.5	0.007	0.10	0.026	0.034	C3 − C	−0.037	−0.010	−0.027

conditions were set identical to event B. Results from event simulation A1 suggest that the flood response amount of event A would be much less, and also very similar to that of event B, if the antecedent conditions of B were used. This confirms that antecedent conditions play a dominant role in varied response of events A and B and could be an important factor in determining a wide range of streamflow responses to hurricane-season storms in general. It should be noted, however, that event simulation A1 does not fully identify if the moisture deficit near the land surface (say, in the top 25 cm) is the major contributor to differential response or if differences in groundwater table depths are also important. To explore this further, two additional experiments (A2 and A3) were conducted. The simulation configuration of A2 was set exactly the same as A, but the groundwater initial condition was set identical to that of event B. The simulated flood response amount for event A2, which only marginally differed from that of event A, indicated that groundwater depth did not play a substantial role in determining varied responses between events A and B. In contrast, event simulation A3, which has the same configuration as A but with surface soil (top 25 cm) moisture identical to B, showed a flood response amount that was more akin to event B, thus confirming that surface soil moisture was the primary driver for the disparity in responses between event A and B. The role of antecedent moisture conditions in varied streamflow responses was also evident for event pairs (20 and 27) and (21 and 39) in Table 1, where streamflow response was also significantly larger when antecedent soil moisture was higher. These results highlight that differences in individual hydrologic stores (unsaturated zone or groundwater) can play as significant a role as differences in total storage in determining varied streamflow response to hurricane-season storms.

We examined variations in surface flow depth, near the land surface saturation (top 25 cm), and in groundwater depth during events A and B to further understand how soil moisture deficit near the land surface influences variability in response, even while groundwater initial conditions have a negligible impact (Fig. 5). For certain periods during both events, simulation results suggested that the top 25 cm was saturated in most of the watershed. However, the groundwater table was never that shallow anywhere in the watershed during the time of saturation (Figs. 5a,b). This indicates that overland flow generated during saturation (shown in Figs. 5c,d) was primarily because of an infiltration excess process resulting from saturation in the near-surface soil. It should be noted that the absence of transient groundwater observation data within the watershed makes it difficult to absolutely confirm that the groundwater table does not reach the land surface during the period when surface soil experiences saturation, as was simulated by the model. However, observed groundwater level time series from a neighboring watershed [North Carolina Division of Water Resources (NCDWR) Caldwell site #F43 × 1; the site is 19.3 km from the LMW outlet; NCDWR 2014] confirmed that the groundwater table never reached the land surface even in the valley floor during the entire observation period (1985–2012). Additionally, soil saturation SS data at the ECONet site (Fig. 3d), which incidentally also exists outside the LMW (see section 2c), confirmed that the near-surface soil moisture did reach saturation during hurricane-season storms, as was also simulated by the model. Because infiltration excess due to near-surface saturation was the cause of overland flow generation

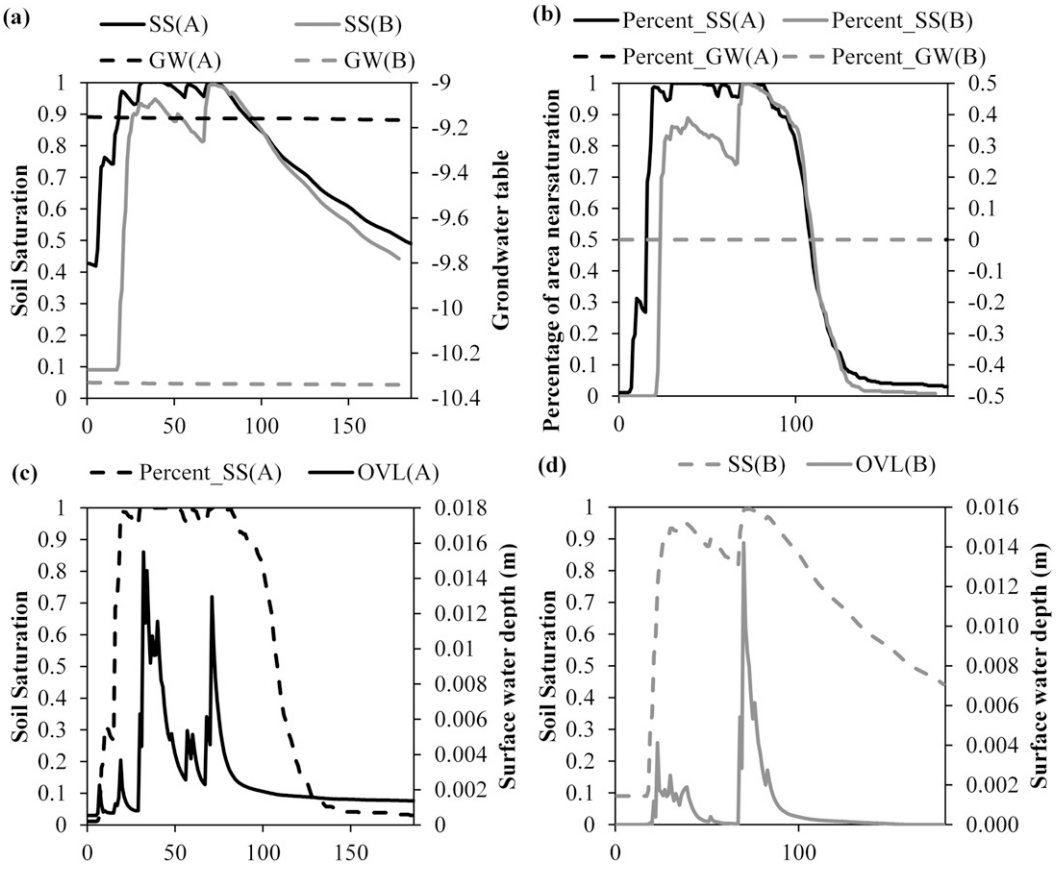

FIG. 5. (a) Average SS and GW for events A and B, (b) percentage of watershed area near saturation (Percent_SS) and area with GW hitting the land surface (Percent_GW) for events A and B, (c) SS and overland flow depth (OVL) for event A, and (d) SS and OVL for event B.

during the two events, lower antecedent soil saturation for event D (Table 3, Fig. 5a) meant that a larger soil moisture deficit had to be satisfied before overland flow can be generated. Hence, antecedent soil saturation conditions near the land surface can play a crucial role in determining surface flow response. Because overland flow contribution to streamflow during events A and B was as large as 97% and 98%, respectively, antecedent soil moisture conditions near the land surface ended up being the primary determinant of the varied response in events A and B.

To evaluate the role of near–land surface moisture deficits on variable responses due to large hurricane-season storms in general, the correlation coefficient between streamflow amount and effective precipitation size, evaluated here as $(p - d)$, where d is the moisture deficit in the top 25 cm, was compared to the correlation between event_Q and p for all top-50 hurricane-season events. Improved R^2 of 0.77 for event_Q versus eff_p (Fig. 6b) with respect to event_Q versus p (Fig. 6a) indicates that soil moisture deficit is indeed an important determinant in variability of streamflow response and hence also on its predictability. Notably, R^2 between event_Q versus eff_p for the case when eff_p is evaluated as $(p - d)$, where d is the moisture deficit defined by groundwater table depth, reduced to 0.44, thus reconfirming that groundwater level did not play a substantial role in variability of streamflow response and hence in its predictability.

It should be noted that the differences in antecedent soil saturation conditions, which influenced the streamflow response, may themselves be controlled by previous precipitation. To explore this further, R^2 values between antecedent soil moisture and total precipitation amount in the previous N days (where N is a positive integer) were evaluated. Results reveal that precipitation in the previous 1, 4, 8, 15, and 30 days explained 6.4%, 22.4%, 24.8%, 22.7%, and 16.6% of the variance in antecedent soil moisture, respectively. Sizable R^2 values indicate that precipitation history did influence the antecedent soil moisture and hence hydrologic response to large storms. Furthermore, a maximum R^2 for $N = 8$ days

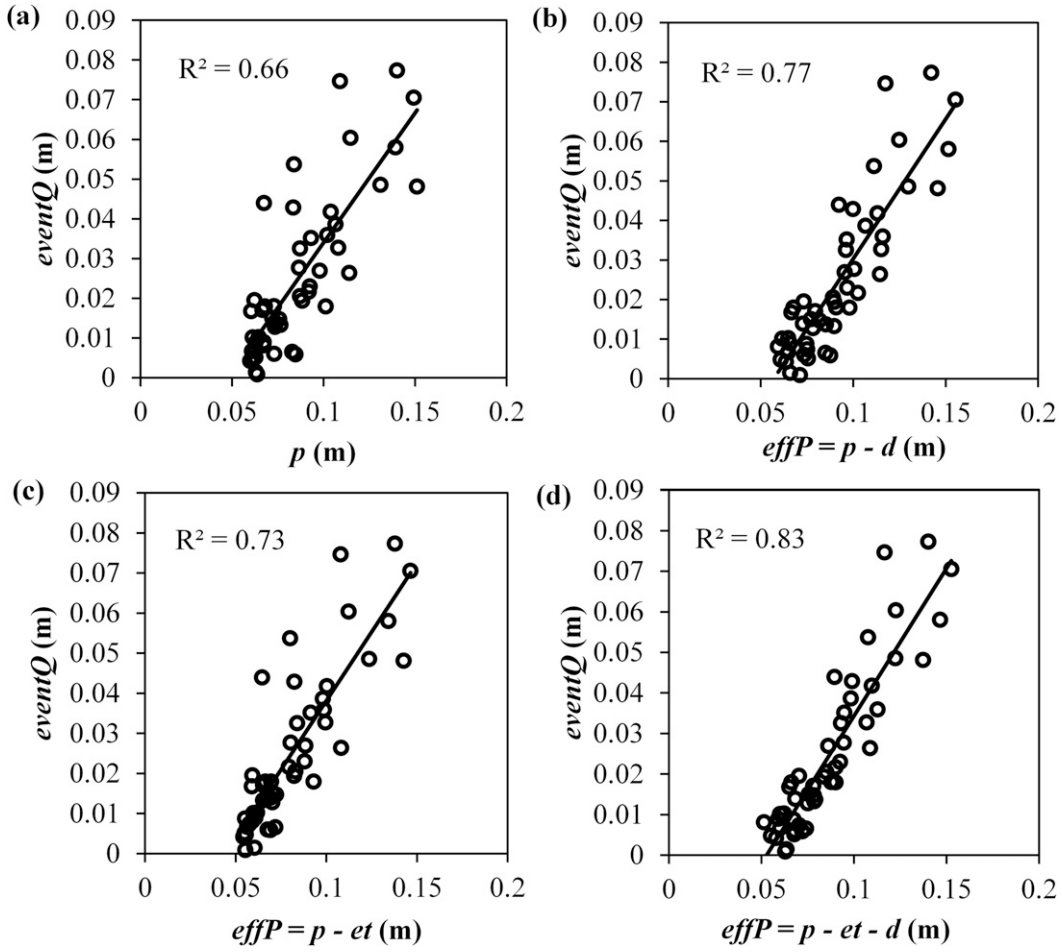

FIG. 6. Linear regression between (a) precipitation and streamflow magnitudes, (b) effective precipitation ($\text{eff}_p = p - d$) and event_Q, (c) effective precipitation ($\text{eff}_p = p - \text{et}$) and event_Q, and (d) effective precipitation ($\text{eff}_p = p - \text{et} - d$) and event_Q. Variable d is the moisture deficit in top 25 cm of soil, and et is the total evapotranspiration during an event.

suggests that the soil moisture memory of the watershed was approximately one week.

b. *Role of evapotranspiration on variable streamflow response*

Comparison of water budget partition in events C and D (see Table 3) shows that evapotranspiration loss plays an important role in the disparity in streamflow response. Evapotranspiration during event D (0.031 m) was markedly larger than during event C (0.007 m). It is to be noted again that et is the total evapotranspiration during the streamflow event, which spans from the start of the storm to the time by which the generated streamflow recession limb has flattened. Notably, evapotranspirative losses during the storm periods are relatively small (0.002 and 0.006 m for events C and D, respectively), and hence, the marked difference in et between the two events is because of losses that happen after the storm, a major component of which is due to transpiration of infiltrated water in the root zone. The difference in et rate during poststorm periods is attributable to favorable meteorological (higher temperature and radiation conditions) and ecological (higher leaf area index) conditions in August relative to November (when event C happened). It is to be noted that antecedent conditions for events C and D were also different and could also play a role in differential responses by influencing both et and del_S. To isolate the influence of meteorological conditions and vegetation states on et, a new event simulation, C1, was conducted. Event C1 replicates event C, but with an assumption that it happens in August (at the same time as event D). This means that meteorological and vegetation conditions during C1 were the same as that during event D.

Expectedly, et for event C1 was much larger than in event C, thus reinforcing the fact that the difference in et between events C and D was largely due to their timing and differences in potential evapotranspiration. Notably, a relatively large evapotranspiration loss in C1 in relation to event D does not translate to a very small flood response, as was the case in event D. This suggests that antecedent conditions could also be playing a role in differential response. To evaluate the role of antecedent conditions, event simulation C2 was conducted with exactly the same modeling configuration as event C, but with antecedent conditions that were set identical to event D. Results suggest that while event_Q in this case is relatively smaller than event C, it is still markedly different than event_Q in event D. The combined effect of differences in antecedent conditions and et was evaluated by event simulation C3, which has the same timing and antecedent conditions as event D. The simulated flood response amount for event C3 now only marginally differed from that of event D. This indicates that both et and moisture deficit contributed to varied responses between events C and D. The combined effect of et and moisture deficit is evident in the event pair 15 and 26 (see Table 1), for which the streamflow responses are almost the same even though event 26 had a much higher antecedent soil moisture. This is because of much larger et during the postevent streamflow recession period of event 26, as it occurs in July when potential evapotranspiration rates are relatively larger.

To evaluate the role of differences in et on variable flood responses due to large hurricane-season storms, correlation coefficients between event_Q and eff_p were evaluated for the largest 50 hurricane-season storms during the simulation period. Here eff_p is calculated as $(p - \text{et})$. Improved R^2 of 0.73 (Fig. 6c) with respect to event_Q versus p (Fig. 6a) indicates that et was indeed an important determinant in variability of streamflow response and hence also on its predictability. It is to be noted that variations in et are often rooted in differences in timing of respective events, as timing determines both the vegetation states and meteorological conditions that are conducive to et. This suggests that variability in flood response due to hurricane-season storms can sometimes be simply related to timing of the event within a year, with a smaller response expected in summer (June–August) when et is as large as 40% of event precipitation.

The integrated role of antecedent conditions and et on the variability of flood response due to the largest 50 hurricane-season storms was further evaluated by recalculating the correlation between event_Q and eff_p, where eff_p is calculated as $(p - \text{et} - d)$. Improved R^2 of 0.83 (Fig. 6d) confirms the potential role of both et and antecedent near-surface soil moisture conditions on the variability of streamflow response amount. Further analyses suggest that the average ''missing'' percentage of precipitation [quantified as $100(1 - \text{event}_Q/p)$] for the largest 50 hurricane-season storms was as large as 74% of the precipitation amount, of which approximately 52% and 22% were lost to soil moisture deficit and evapotranspiration, respectively. The results indicate that antecedent soil moisture was the dominant control on streamflow response. Event-based analyses showed that antecedent soil moisture was the primary control on streamflow response in 28 out of the 50 top hurricane-season storms, while evapotranspirative losses were dominant in 22 storms. Relative dominance of the two controls on streamflow response showed a seasonal trend, with antecedent soil moisture being the dominant control for 73.5% of large hurricane-season storms during August–November. In contrast, evapotranspiration was the main determinant in 87.5% of the large hurricane-season storms between June and July.

4. Conclusions and synthesis

This paper evaluates the extent of variability in streamflow response due to large hurricane-season storms and examines the role of transient hydrologic controls on said variability. Analyses were conducted based on model simulation results obtained from a physically based integrated hydrologic model, PIHM, which was validated for multiple states within the Lake Michie watershed, including streamflow hydrograph, runoff ratio, groundwater table elevation, soil moisture, and ranges of evapotranspiration. To confirm the applicability of the model for analyses of variability in streamflow response, ranks of predicted streamflow responses were validated. The validated model was then used to perform nested control event simulations to quantify the variability in streamflow response and to identify and isolate the role of hydrologic controls on different water stores during storm events. Analyses suggest that hurricane-season storms of similar size could generate a considerable range of streamflow responses (more than 100% difference), thus highlighting that it is not reliable to use storm size alone to predict the streamflow response and the consequent flood. Event simulations suggest that the dominant controls on the variability of streamflow amount were soil saturation near the ground surface and evapotranspirative losses, which are in turn influenced by meteorological conditions and vegetation states. Generally, higher antecedent topsoil saturation would lead to generation of larger streamflow in response to events of similar sizes. Also, because meteorological conditions and ecohydrologic functions of vegetation follow a seasonal variation,

streamflow response shows a strong dependence on timing of the event within a year. For example, streamflow amount, in response to events of similar sizes, is much less for events that happen in July with respect to the ones that happen in November. Notably, groundwater contribution on streamflow amount under hurricane-season storms is negligible. The role of identified controls on varied streamflow responses for a wider set of hurricane-season storms was evaluated by calculating the predictability of streamflow response size after accounting for the role of controls. Increased correlation between streamflow response size and effective storm size, which accounts for the role of controls, compared to that between streamflow amount and precipitation alone further reinforced the role of individual hydrologic controls. Between antecedent topsoil saturation and postevent evapotranspiration, the former was identified as the dominant control on streamflow response amount. However, evapotranspiration was still a primary determinant on streamflow response, especially during June and July.

Information regarding the dominant controls on variability of streamflow response can be used to help prioritize resources for field campaigns and observation systems. For example, distributed measurements of soil moisture, which play a crucial role in determining flood response, can be used in assimilation of antecedent soil moisture states, regionalization of relevant sensitive model parameters, and validation of model results, thus leading to an improved predictability and reduced uncertainty in estimation of flood response to large hurricane-season storms. In contrast, a much-refined groundwater network, although important, might not sufficiently improve the prediction of flood response to hurricane-season storms. Knowledge of process controls and antecedent conditions can also be used to aid in risk management by providing look-up diagrams to quickly evaluate flood responses, given prior information about hurricane storm size. This may be realized through development of a streamflow response map for a range of antecedent conditions, timings of hurricane storms, and event sizes in a watershed. One simplistic but representative example of a look-up diagram is shown in Fig. 7, which shows streamflow response to three hurricane storms of varying sizes, happening at different times (June, September, and November), and during dry, intermediate, and wet antecedent states. A look-up diagram of this sort, with responses mapped at finer resolutions and for a wide range of conditions, could be used by resource managers to easily estimate the flood response size due to an impending hurricane storm. In addition, comparison of look-up diagrams or storm-response maps among different watersheds can also provide information about which watershed is more vulnerable to events of a particular size. It should be noted that the two dominant controls on the variability in flood response documented here—antecedent soil moisture and evolving vegetation states and meteorological conditions—can both be estimated using remote sensing data. This points to the potential for using satellite data to improve flood prediction due to hurricane-season storms. It is to be noted that the dominant hydrologic controls identified in LMW might not be applicable in all the southeastern U.S. watersheds because of differences in topographic, physiographic, and other hydrogeologic properties such as soil drainage parameters and vegetation types, all of which can influence infiltration and evapotranspiration rates. In addition, while the validation process took advantage of available hydrologic datasets within and around the Lake Michie watershed, further confidence in the model performance and analyses could be built by observing additional hydrologic variables for validation, such as transient groundwater depth and evapotranspiration.

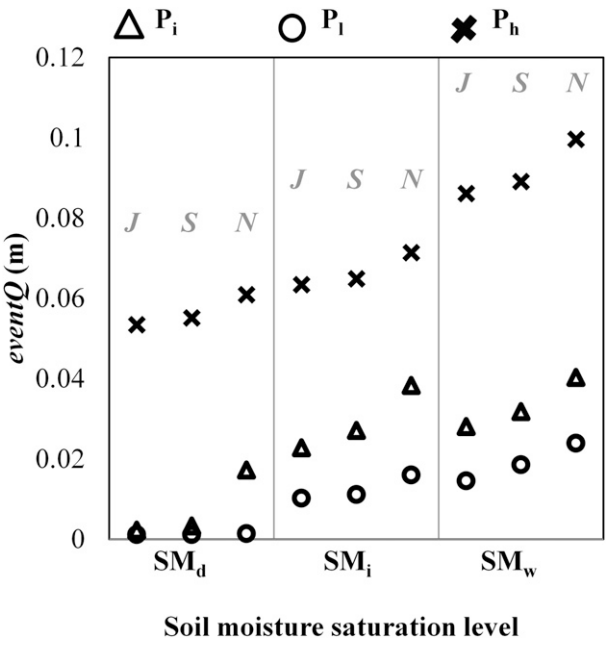

FIG. 7. Streamflow magnitude under different antecedent soil moisture conditions in topsoil layer (25 cm), timing of event, and storm size. Variables SM_d, SM_i, and SM_w indicate dry, intermediate, and wet topsoil saturation conditions, respectively; J, S, and N indicate July, September, and November, respectively; and p_i, p_l, and p_h indicate intermediate, low, and high precipitation magnitudes, respectively.

Acknowledgments. This study was supported by Grant NSF-EAR1331846 from Calhoun Critical Zone Observatory, an Ecosystem and Water Working Group seed

grant from the Nicholas Institute, and the Duke University start-up fund for new faculty. We would also like to thank all three anonymous reviewers for their constructive comments that greatly improved this manuscript.

REFERENCES

Ashley, S. T., and W. S. Ashley, 2008: Flood fatalities in the United States. *J. Appl. Meteor. Climatol.,* **47,** 805–818, doi:10.1175/2007JAMC1611.1.

Bhatt, G., M. Kumar, and C. J. Duffy, 2008: Bridging the gap between geohydrologic data and integrated hydrologic modeling. *Proc. iEMSs 2008: Int. Congress on Environmental Modelling and Software,* Vol. 2, Barcelona, Spain, International Environmental Modelling and Software Society, 743–750. [Available online at www.iemss.org/iemss2008/uploads/Main/Vol2-iEMSs2008-Proceedings.pdf.]

——, ——, and ——, 2014: A tightly coupled GIS and distributed hydrologic modeling framework. *Environ. Modell. Software,* **62,** 70–84, doi:10.1016/j.envsoft.2014.08.003.

Blake, E. S., C. W. Landsea, and E. J. Gibney, 2007: The deadliest, costliest, and most intense United States tropical cyclones from 1851 to 2006 (and other frequently requested hurricane facts). NOAA Tech. Memo. NWS TPC-5, 43 pp. [Available online at www.nhc.noaa.gov/pdf/NWS-TPC-5.pdf.]

Carney, C. B., and A. V. Hardy, 1967: North Carolina hurricanes: A listing and description of tropical cyclones which have affected the state. Rev. ed. U.S. Government Printing Office, 40 pp.

Castillo, V. M., A. Gomez-Plaza, and M. Martinez-Mena, 2003: The role of antecedent soil water content in the runoff response of semiarid catchments: A simulation approach. *J. Hydrol.,* **284,** 114–130, doi:10.1016/S0022-1694(03)00264-6.

Changnon, S., 2009: Characteristics of severe Atlantic hurricanes in the United States: 1949–2006. *Nat. Hazards,* **48,** 329–337, doi:10.1007/s11069-008-9265-z.

——, and J. Changnon, 1992: Temporal fluctuations in weather disasters: 1950–1989. *Climatic Change,* **22,** 191–208, doi:10.1007/BF00143027.

Dale, V. H., and Coauthors, 2001: Climate change and forest disturbances: Climate change can affect forests by altering the frequency, intensity, duration, and timing of fire, drought, introduced species, insect and pathogen outbreaks, hurricanes, windstorms, ice storms, or landslides. *BioScience,* **51,** 723–734, doi:10.1641/0006-3568(2001)051[0723:CCAFD]2.0.CO;2.

Easterling, D. R., G. A. Meehl, C. Parmesan, S. A. Changnon, T. R. Karl, and L. O. Mearns, 2000: Climate extremes: Observations, modeling, and impacts. *Science,* **289,** 2068–2074, doi:10.1126/science.289.5487.2068.

Elsenbeer, H., D. Lorieri, and M. Bonell, 1995: Mixing model approaches to estimate storm flow sources in an overland flow-dominated tropical rain forest catchment. *Water Resour. Res.,* **31,** 2267–2278, doi:10.1029/95WR01651.

Elsner, J. B., 2007: Granger causality and Atlantic hurricanes. *Tellus,* **59A,** 476–485, doi:10.1111/j.1600-0870.2007.00244.x.

Emanuel, K. A., 1987: The dependence of hurricane intensity on climate. *Nature,* **326,** 483–485, doi:10.1038/326483a0.

——, R. Sundararajan, and J. Williams, 2008: Hurricanes and global warming: Results from downscaling IPCC AR4 simulations. *Bull. Amer. Meteor. Soc.,* **89,** 347–367, doi:10.1175/BAMS-89-3-347.

Goldenberg, S. B., C. W. Landsea, A. M. Mestas-Nuñez, and W. M. Gray, 2001: The recent increase in Atlantic hurricane activity: Causes and implications. *Science,* **293,** 474–479, doi:10.1126/science.1060040.

Hardy, A. V., and C. B. Carney, 1963: North Carolina hurricanes: A descriptive listing of tropical cyclones which have affected the state. U.S. Government Printing Office, 26 pp.

Jones, J. P., E. A. Sudicky, and R. G. McLaren, 2008: Application of a fully-integrated surface–subsurface flow model at the watershed-scale: A case study. *Water Resour. Res.,* **44,** W03407, doi:10.1029/2006WR005603.

Knutson, T. R., and R. E. Tuleya, 2004: Impact of CO_2-induced warming on simulated hurricane intensity and precipitation: Sensitivity to the choice of climate model and convective parameterization. *J. Climate,* **17,** 3477–3495, doi:10.1175/1520-0442(2004)017<3477:IOCWOS>2.0.CO;2.

Kopec, R. J., and J. W. Clay, 1975: Climate and air quality. *North Carolina Atlas: Portrait of a Changing Southern State,* J. W. Clay, D. M. Orr Jr., and A. W. Stuart, Eds., University of North Carolina Press, 92–111 pp.

Kumar, M., 2009: Toward a hydrologic modeling system. Ph.D. thesis, The Pennsylvania State University, 274 pp.

——, G. Bhatt, and C. J. Duffy, 2009a: An efficient domain decomposition framework for accurate representation of geodata in distributed hydrologic models. *Int. J. Geogr. Inf. Sci.,* **23,** 1569–1596, doi:10.1080/13658810802344143.

——, C. J. Duffy, and K. M. Salvage, 2009b: A second-order accurate, finite volume-based, integrated hydrologic modeling (FIHM) framework for simulation of surface and subsurface flow. *Vadose Zone J.,* **8,** 873–890, doi:10.2136/vzj2009.0014.

——, G. Bhatt, and C. J. Duffy, 2010: An object-oriented shared data model for GIS and distributed hydrologic models. *Int. J. Geogr. Inf. Sci.,* **24,** 1061–1079, doi:10.1080/13658810903289460.

Landsea, C., 2007: Counting Atlantic tropical cyclones back to 1900. *Eos, Trans. Amer. Geophys. Union,* **88,** 197–202, doi:10.1029/2007EO180001.

Mann, M. E., and K. A. Emanuel, 2006: Atlantic hurricane trends linked to climate change. *Eos, Trans. Amer. Geophys. Union,* **87,** 233–241, doi:10.1029/2006EO240001.

Mitchell, K. E., and Coauthors, 2004: The multi-institution North American Land Data Assimilation System (NLDAS): Utilizing multiple GCIP products and partners in a continental distributed hydrological modeling system. *J. Geophys. Res.,* **109,** D07S90, doi:10.1029/2003JD003823.

MRLC, cited 2013: National Land Cover Database 2006. [Available online at www.mrlc.gov/nlcd2006.php.]

NCDC, cited 2014: North Carolina hurricane events. Storm events database. [Available online at www.ncdc.noaa.gov/stormevents/listevents.jsp?beginDate_mm=01&beginDate_dd=01&beginDate_yyyy=1996&endDate_mm=04&endDate_dd=30&endDate_yyyy=2013&eventType=%28Z%29+Hurricane+%28Typhoon%29&county=ALL&zone=ALL&submitbutton=Search&statefips=37%2CNORTH+CAROLINA.]

NCDWR, cited 2014: Ground water level database detail. North Carolina Division of Water Resources. [Available online at http://ncwater.org/Data_and_Modeling/Ground_Water_Databases/leveldetail.php?quado=F**43X1.]

NOAA, cited 2013a: Preliminary report: Hurricane Fran. [Available online at www.nhc.noaa.gov/1996fran.html.]

——, cited 2013b: Historical hurricane tracks. [Available online at http://coast.noaa.gov/hurricanes/.]

Pielke, R. A., C. Landsea, M. Mayfield, J. Laver, and R. Pasch, 2005: Hurricanes and global warming. *Bull. Amer. Meteor. Soc.,* **86,** 1571–1575, doi:10.1175/BAMS-86-11-1571.

Qu, Y., and C. J. Duffy, 2007: A semidiscrete finite volume formulation for multiprocess watershed simulation. *Water Resour. Res.,* **43,** W08419, doi:10.1029/2006WR005752.

Refsgaard, J. C., and B. Storm, 1996: Construction, calibration and validation of hydrological models. *Distributed Hydrological Modelling,* M. Abbott and J. Refsgaard, Eds., Springer, 41–54.

Salinger, M. J., 2005: Climate variability and change: Past, present and future—An overview. *Climatic Change,* **70,** 9–29, doi:10.1007/s10584-005-5936-x.

Saunders, M. A., R. E. Chandler, C. J. Merchant, and F. P. Roberts, 2000: Atlantic hurricanes and NW Pacific typhoons: ENSO spatial impacts on occurrence and landfall. *Geophys. Res. Lett.,* **27,** 1147–1150, doi:10.1029/1999GL010948.

SCONC, cited 2014a: Tropical cyclones that have affected the southeastern US. State Climate Office of North Carolina. [Available online at www.nc-climate.ncsu.edu/climate/hurricanes/affecting.php?state=NC&buffer=150.]

——, cited 2014b: NC CRONOS Database: North Durham Water Reclamation Facility (DURH). State Climate Office of North Carolina. [Available online at http://hatteras.meas.ncsu.edu/cronos/?station=DURH&temporal=daily.]

Soil Survey Staff, cited 2013: Web soil survey. Natural Resources Conservation Service, United States Department of Agriculture. [Available online at http://websoilsurvey.nrcs.usda.gov/.]

Stoy, P. C., and Coauthors, 2006: Separating the effects of climate and vegetation on evapotranspiration along a successional chronosequence in the southeastern US. *Global Change Biol.,* **12,** 2115–2135, doi:10.1111/j.1365-2486.2006.01244.x.

Sturdevant-Rees, P., J. A. Smith, J. Morrison, and M. L. Baeck, 2001: Tropical storms and the flood hydrology of the central Appalachians. *Water Resour. Res.,* **37,** 2143–2168, doi:10.1029/2000WR900310.

Tramblay, Y., C. Bouvier, C. Martin, J.-F. Didon-Lescot, D. Todorovik, and J.-M. Domergue, 2010: Assessment of initial soil moisture conditions for event-based rainfall–runoff modelling. *J. Hydrol.,* **387,** 176–187, doi:10.1016/j.jhydrol.2010.04.006.

Weaver, J. C., 1994: Sediment characteristic and sedimentation rates in Lake Michie, Durham County, North Carolina, 1990–92. USGS Water-Resources Investigations Rep. 94-4123, 38 pp.

Webster, P. J., G. J. Holland, J. A. Curry, and H.-R. Chang, 2005: Changes in tropical cyclone number, duration, and intensity in a warming environment. *Science,* **309,** 1844–1846, doi:10.1126/science.1116448.

Wood, E. F., 1976: An analysis of the effects of parameter uncertainty in deterministic hydrologic models. *Water Resour. Res.,* **12,** 925–932, doi:10.1029/WR012i005p00925.

Xia, Y., and Coauthors, 2012: Continental-scale water and energy flux analysis and validation for the North American Land Data Assimilation System project phase 2 (NLDAS-2): 1. Intercomparison and application of model products. *J. Geophys. Res.,* **117,** D03109, doi:10.1029/2011JD016048.